

Development and design of a drive unit enabling electrochemical orbiting with high dynamics

Oliver Georgi¹, Hendrik Rentzsch¹, René Schoesau¹, Jan Edelmann¹, Gunnar Meichsner¹

¹Fraunhofer Institute for Machine Tools and Forming Technology IWU, Reichenhainer Str. 88, 09126 Chemnitz, Germany

Submitting author. Tel.: +49 371 5397 1457; fax: +49 371 5397 61457. E-mail address: oliver.georgi@iwu.fraunhofer.de

Abstract

Electrochemical machining is a suitable process for micro and precision manufacturing. To overcome several disadvantages like geometrical restrictions of the workpieces due to the uniaxial sinking the paper presents a new approach. The common kinematic is sequential or continuously superimposed by an orbiting movement of the workpiece which is defined as a circular translation. However using conventional machine components limits the orbiting frequency to a maximum of 2 Hz. The paper shows the development and design of a drive unit enabling electrochemical orbiting up to 50 Hz. To reach this goal a unique kinematic concept was carried out including an adaptive unbalance compensation for different workpiece weights and the movable orbiting radius.

Machine tools, electrochemical machining, kinematic

1. Introduction

Electrochemical machining (ECM) is well-established for the machining of hard and difficult-to-machine materials. Over the years, there has been increasing importance in the field of precise complete machining of complex components [1]. Regarding the common operating mode characterised by uniaxial sinking, several disadvantages and limitations like rounded edges and a limited 3 dimensional imaging accuracy occur. This paper introduces a new approach of an orbiting process kinematic enabled through a high dynamic drive unit. This eliminates restrictions caused by the conventional process kinematic and allows enabling machining of new geometrical features to use ECM for complex workpieces. Thus EC-Orbiting opens up new fields of application for this technology.

The idea of EC-Orbiting is the sequential or continuous superposition of the lowering movement of the electrode with an orbital motion (circular translation) of the workpiece. Aim of the research was to develop a drive unit executing the orbiting with up to 50 Hz while maintaining excellent path accuracy to provide high removal rate and imaging accuracy.

2. Technology

ECM processes are based on the anodic dissolution of metallic workpieces due to the transport of electric charge between cathode and anode using an electrolyte [2, 3]. Advantages include the possibility of machining hard and difficult-to-machine materials as well as burr-free machining with high surface quality and without thermal or mechanical influence on the workpiece structure.

2.1. Precise electrochemical machining PECM

Precise electrochemical machining (PECM) is a modification of ECM using pulsed current combined with an oscillating tool electrode [4, 5]. This enables the reduction of the working gap, consequently increasing the precision of machining due to

higher localization of the current density. The principle of PECM is shown in figure 1.

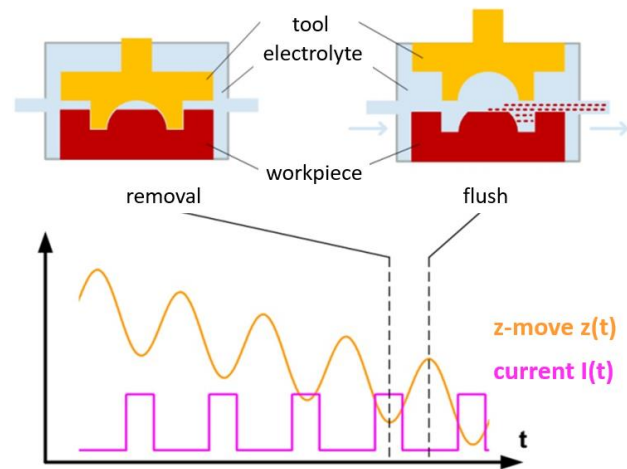


Figure 1: Principle and phases of Precise Electrochemical Machining

The current pulse is carried out during a minimum of the working gap. Concerning the electrolyte saturation the oscillating motion permits excellent flushing conditions in case of the opened working gap at maximum distance between electrode and workpiece [6]. This characteristic leads to a combination of excellent imaging accuracy combined with high removal rates. Common parameters for PECM are a frequency of about 50 Hz and a stroke of 0.4 mm.

2.2. EC Orbiting

As can be seen in figure 2, the orbiting movement describes a circular translation without rotation. EC-Orbiting adopts the principle of an oscillating working gap for circumferential material removal. Thus the workpiece describes the orbital motion sequentially or continuously superimposing the electrodes lowering movement. The feed direction is defined by the orbiting radius.

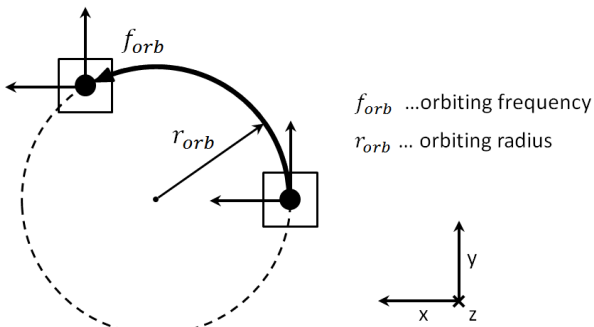


Figure 2: Principle of the orbiting movement

In this way EC-Orbiting embraces the advantages of PECM. Additionally the need for complex tool geometry decreases due to the ability of kinematic shape generation.

Using EC-Orbiting it is possible to create rotationally symmetric free form contours, sharp edges at graded parts or even undercuts like grooves as can be seen Figure 3.

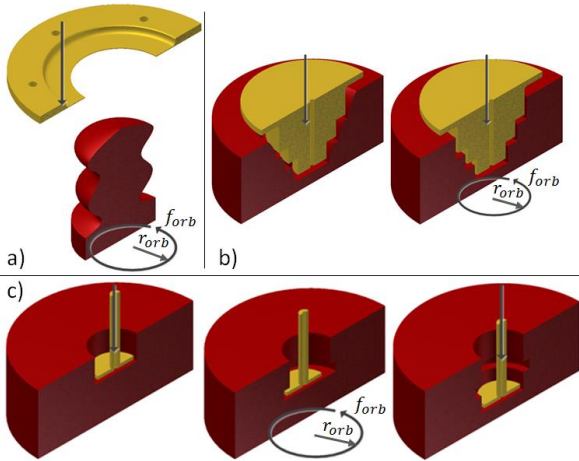


Figure 3: New fields of application due to EC-Orbiting: a) kinematic generated free form parts, b) graded parts, c) undercuts

Preliminary technological investigations showed the potential of EC-Orbiting. Using an existing x-y machining table the presented use cases where executed under a limited orbiting frequency of maximum 2 Hz.

Figure 4 shows the experimental setup as well as a specimen of the application of EC-Orbiting for circumferential material removal to generate undercuts inside a borehole.

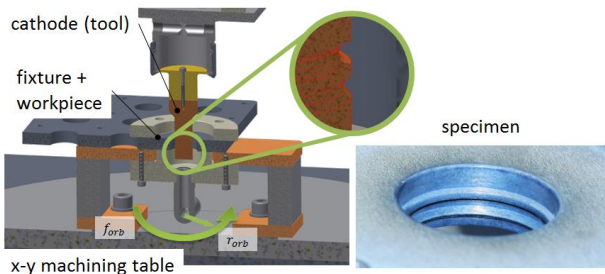


Figure 4: Circumferential material removal generating undercuts

The preliminary investigations provided general evidence for the technical feasibility of EC-Orbiting, but questions regarding precision, removal rate and surface quality remained due to the limited orbiting frequency.

Regarding EC-Orbiting each orbiting cycle represents a single cut. Therefore low orbiting frequencies cause a high local erosion time. Executing EC-Orbiting with a small working gap during such long removal periods, the chemical electrolyte

parameters deteriorate as a consequence of the saturation effect. Without electrolyte exchange, material removal stops after about 10 to 50 ms.

With a higher orbiting frequency of 50 Hz, the removal time decreases to approximately 3 to 10 ms. Between each local ablation, the electrolyte is renewed due to the orbital motion.

If the removal rate is to be increased at low orbiting frequencies, the individual removal for each cut has to be increased. For periodic ECM processes enhancing the general removal rate requires an increase of the individual removal rate for each cut. For low orbiting frequencies a high single cut removal rate leads to a larger working gap due to the distribution of the electric fields and thus to a reduction of the possible imaging accuracy as shown in Figure 6. Therefore only high frequent EC-Orbiting can be executed with a small working gap combining high imaging accuracy with high removal rates.

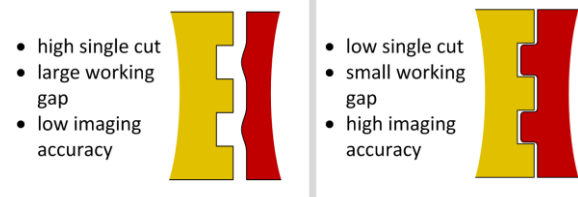


Figure 5: Relationship between gap width, individual removal and imaging accuracy

Following [7, 8] the imaging accuracy s is approximated via the single cut and in analogy to the PECM process according to the equation

$$s = \frac{\left(\frac{dr_{orb}}{dt}\right) \cdot k_{PECM}}{f_{orb}} \quad (1)$$

The technology factor k_{PECM} describes the relationship between individual ablation volume and imaging accuracy. The factor can only be obtained from technological experiments in frequency ranges in which the actual erosion time corresponds to the theoretical erosion time. The existing experimental device with its maximum frequency of 2 Hz does not reach these ranges. The technology factor of 5 used for EC-Orbiting is therefore adopted from experiments with the already established PECM and is an approximation based on the analogies of both processes.

Figure 6 shows the imaging accuracy as a function of the orbiting frequency for various average removal rates as a function of average radius feed rates.

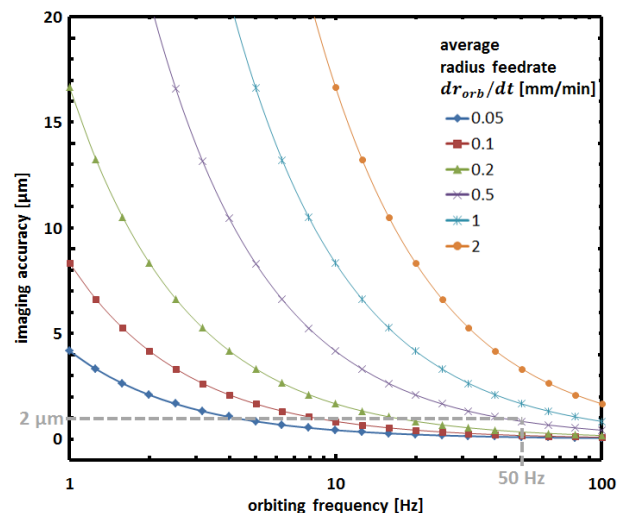


Figure 6: Imaging accuracy as a function of the orbiting frequency

For low removal rates of e.g. 0.1 mm/min the desired imaging accuracy of 2 μm is theoretically already achieved at frequencies of about 4 Hz. To reach an accuracy of 2 μm in combination with industry-suitable feed rates of 1 mm/min or higher, an orbiting frequency of 50 Hz is necessary. A further increase is expected, according to the current state of knowledge, to result only in small improvements in accuracy. Consequently the industrial application of EC-Orbiting depends on the availability of a drive unit enabling orbital motion with high frequencies.

3. Development of the drive unit

Table 1 shows an extract of the main technical specifications for the drive unit to be integrated in PEM Center 8000.

Table 1: Specifications of the drive unit

available space	500 mm x 500 mm x 500 mm
workpiece dimensions	300 mm x 300 mm x 200 mm max. 5 kg
orbiting frequency f_{orb}	0.1 – 50 Hz (closed-loop)
orbiting radius r_{orb}	0 – 10 mm
radius federate dr_{orb}/dt	0.001 mm/min
forces direction z	10 kN
forces direction x,y	1 kN

Key aspects for the development of the drive unit are:

- the high main forces in z-direction caused by the process
- outstanding dynamics caused by the orbiting movement
- high requirements for path accuracy because of the direct affect to workpiece geometry

The radial accelerations can be described by

$$a_{rad} = r_{orb} \cdot \omega^2 = r_{orb} \cdot (2 \cdot \pi \cdot f_{orb})^2. \quad (2)$$

Figure 7 shows the radial acceleration concerning the specifications of the drive unit.

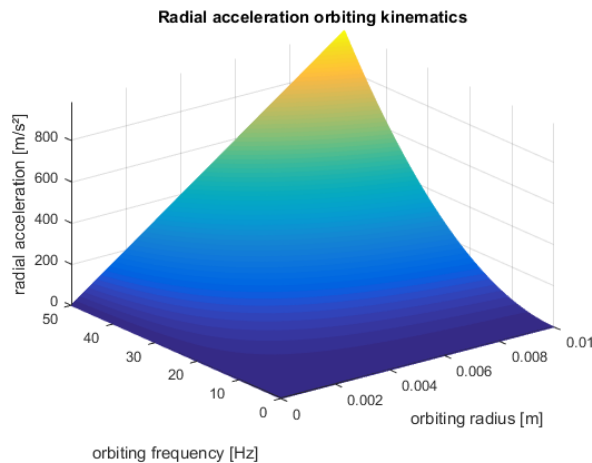


Figure 7: Radial acceleration as a function of orbiting radius and frequency

Applying the maximum parameters in table 1 to equation (2) shows, that radial acceleration up to 986 m/s^2 can occur.

Because common drive systems do not fulfill the posted requirements an innovative drive unit with a specific kinematic structure for high dynamic orbital motion was developed.

3.1. Concept of the kinematics

Figure 8 shows the principle kinematic concept.

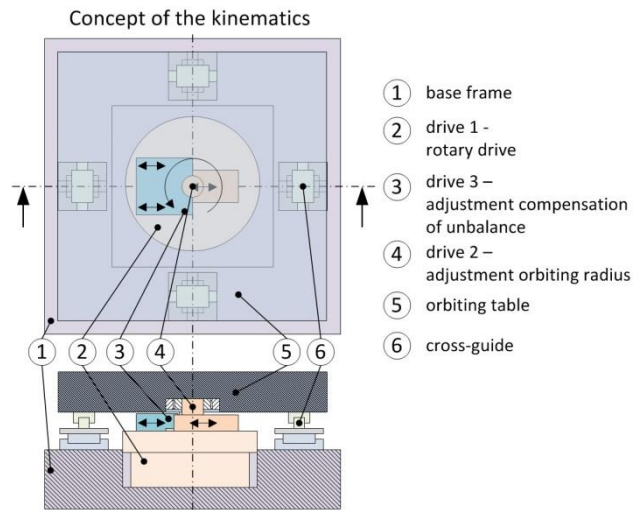


Figure 8: Concept of the kinematics

Drive 1 generates the orbiting frequency. Drive 2 shifts the radius of the orbiting movement similar to an adjustable exzentric. The third drive moves the balancing mass compensating the static unbalance generated by the orbital motion.

The main drive 1 is a belt drive rotating a hollow shaft. Drive 2 and drive 3, situated on top of drive 1, generate linear motions. It is not possible to directly integrate actuators due to the rotational speed of up to 3000 min^{-1} representing the maximum orbiting frequency of 50 Hz. This was addressed by developing a mechanism based on a worm gear actuating a ball screw which provides a linear motion koaxial to the hollow shaft axis. This motion is decoupled from the orbiting frequency and transmitted to the rotating part by a crank to generate linear movement in the desired direction. Drive 3 is a similar mechanism interlaced in drive 2. Figure 9 shows the kinematic diagram of the two axes.

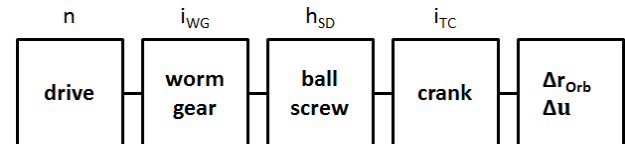


Figure 9: Structural setup for drive 2 and drive 3

This multi-level gear leads to a high transmission ratio, providing a low feed rate and a high motion resolution for orbiting radius regulation and unbalance compensation. Because of the crank, the transmission ratio is not constant over the travel which is being accounted for in an according transfer function.

Furthermore there are three miniaturized cross guides displaced by 120°, which allow planar motion without rotation of the table while providing direction independent inertia.

3.2. Dimensioning of the compensation of the unbalance

Figure 10 displays the different masses during EC-Orbiting. For orbiting motions with an increasing radius a static unbalance force occurs [9]. The unbalance force is described by

$$F_{orb} = (m_{table} + m_{setup}) \cdot r_{orb} \cdot \omega^2. \quad (3)$$

This force is related to the frequency, the radius of the orbiting motion and the total orbiting mass. This mass consists of the orbiting table as well as the workpiece including the fixtures. In consequence of the dissolution of material removal the mass of the workpiece decreases and accordingly the

unbalance force changes. Thus an adaptive compensation of the unbalance during the process was developed.

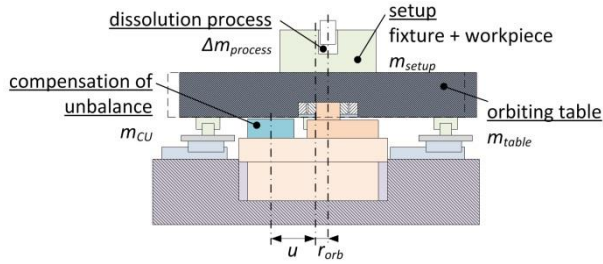


Figure 10: Masses during EC-Orbiting

Concerning the described masses the unbalance force F_{orb} and the compensation force F_{CU} are determined by

$$F_{orb} = (m_{table} + m_{setup} + \Delta m_{process}) \cdot r_{orb} \cdot \omega^2 \quad (4)$$

$$F_{CU} = m_{CU} \cdot u \cdot \omega^2.$$

The equations of these two forces lead to a transfer function for the position u of the balance mass according to

$$u = \frac{(m_{table} + m_{setup} + \Delta m_{process})}{m_{CU}} \cdot r_{orb}. \quad (5)$$

To couple the compensation force a package of springs is applied, which is integrated between the orbiting masses and the compensation device, see Figure 11.

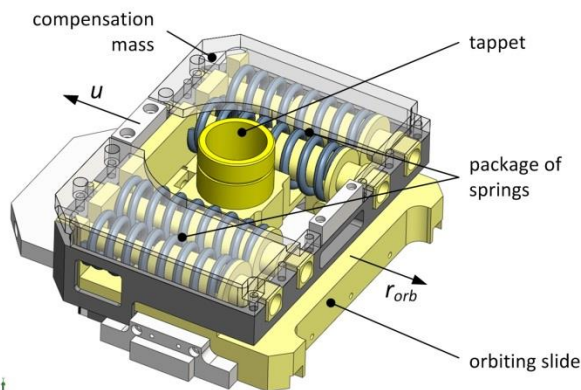


Figure 11: Design of the radius adjustment and the coupled compensation of the unbalance

In addition to the compensation of the static unbalance an adjustment regarding dynamic unbalance is necessary [9]. Shape and arrangement of workpiece and fixtures lead to a displacement of the centre of mass of the orbiting mass. This induces a dynamic unbalance and a high inertia around the z-axis. Therefore an adjustment of the centre of gravity is implemented, which contains two movable masses on the backside of the orbiting table.

3.3. Structural setup of the complete orbiting unit

Figure 12 shows a general view of the orbiting unit consisting of a monolithic base frame which carries all subassemblies. The main focus during the mechanical development of the drive unit for EC-Orbiting was to achieve a compact design in combination with a stiff structure.

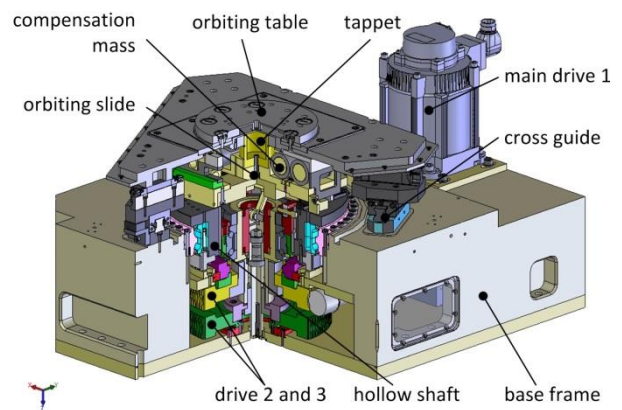


Figure 12: Design of the complete orbiting unit

4. Conclusion

The paper presents an innovative approach for a new modification of ECM called EC-Orbiting using a high dynamic drive unit that enables the electrochemical machining for new fields of application. This drive unit generates an orbiting motion of the workpiece up to a frequency of 50 Hz and a radius of up to 10 mm using an innovative kinematic structure. Additionally an adaptive compensation of unbalance guarantees high accuracy and dynamic stability.

Subsequent to assembly and start up experimental investigations regarding path accuracy, compensation of unbalance and load tests will be carried out. In further steps technological experiments to verify the advantages of high dynamic EC-Orbiting will be executed.

Acknowledgements

This research was supported by the German Federal Ministry for Economic Affairs and Energie (BMWi).

References

- [1] Osenbruggen C and Regt C 1985 Electrochemical micromachining *Philips technical review* **42** Nr. 1 pp 22–22
- [2] Hackert-Oschätzchen M, Boenig L, Meichsner G, Zinecker M, Krönert M and Schubert A 2013 Precise Electrochemical Machining of Rotating Workpieces *Proc. of the 9th Int. Symp. on Electrochemical Machining Techn.*
- [3] Schubert A, Meichsner G, Hackert-Oschätzchen M, Martin A and Edelmann J 2012 Micro Wire Cutting by Pulsed Electrochemical Machining *Proc. of the 8th Int. Symp. on Electrochemical Machining Techn.*
- [4] Hackert-Oschätzchen M, Schubert A, Martin A, Winkler S, Kuhn D, Meichsner G, Zeidler H and Edelmann J 2016 Generation of Complex Surfaces by Superimposed Multi-dimensional Motion in Electrochemical Machining *Proc. of the 18th CIRP Conf. on Electro Physical and Chemical Machining* pp 384 - 89
- [5] Klocke F and König W 2007 *Fertigungsverfahren, Band 3* (Berlin Heidelberg, Germany)
- [6] Schubert A, Hackert-Oschätzchen M, Meichsner G, Zinecker M, Edelmann J 2011 Precision and Micro ECM with Localized Anodic Dissolution *Proc. of the 8th Int. Conf. on Industrial Tools and Material Processing Techn.*
- [7] Meichsner G 2018 Entwicklung und Realisierung einer Methode zur Bestimmung von Prozesseingangsgrößen für das elektrochemische Präzisionsabtragen *Scripts Precision and Microproduction Engineering Band 12*
- [8] Hackert-Oschätzchen M, Boenig L, Meichsner G, Zinecker M, Krönert M and Schubert A 2013 Precise Electrochemical Machining of Rotating Workpieces *Proc. of the 9th Int. Symp. on Electrochemical Machining Technology* pp 89 - 100
- [9] Schneider H 2013 *Auswuchttechnik* (Berlin Heidelberg, Germany)